

# High magnetoelectric effect in laminated composites of giant magnetostrictive alloy and lead-free piezoelectric ceramic

Yanmin Jia<sup>a)</sup>

State Key Laboratory of High Performance Ceramics and Superfine Microstructure,  
Shanghai Institute of Ceramics, Chinese Academy of Sciences, Shanghai 201800, China;  
Graduate School of the Chinese Academy of Sciences, Beijing 100039, China;  
and Department of Applied Physics, The Hong Kong Polytechnic University,  
Hung Hom, Kowloon, Hong Kong

Siu Wing Or, Jie Wang, and Helen Lai Wa Chan

Department of Applied Physics, The Hong Kong Polytechnic University, Hung Hom, Kowloon,  
Hong Kong

Xiangyong Zhao and Haosu Luo

Shanghai Institute of Ceramics, Chinese Academy of Sciences, Shanghai 201800, China

(Received 6 July 2006; accepted 13 March 2007; published online 17 May 2007)

Magnetoelectric (ME) laminated composites with all phases environmentally friendly were prepared by sandwiching one layer of thickness-polarized  $(\text{Bi}_{1/2}\text{Na}_{1/2})\text{TiO}_3$ - $(\text{Bi}_{1/2}\text{K}_{1/2})\text{TiO}_3$ - $\text{BaTiO}_3$  lead-free piezoelectric ceramic disk between two layers of thickness-magnetized  $\text{Tb}_{0.3}\text{Dy}_{0.7}\text{Fe}_{1.92}$  giant magnetostrictive alloy disk along the thickness direction. The composites exhibited the maximum ME voltage coefficient of 40.7 mV/Oe with a flat response in the measured frequency range of 0.1–20 kHz under a dc magnetic bias of 5 kOe. The induced ME voltage showed an extremely linear relationship to the applied ac magnetic field with amplitude varying from  $3 \times 10^{-5}$  to 10 Oe over a broad range of dc magnetic bias of 0–5.5 kOe. The high ME effect was analyzed and found to be comparable to most major lead-based ME composites. The present study opens up possibilities for developing green ME devices. © 2007 American Institute of Physics.

[DOI: 10.1063/1.2732420]

## I. INTRODUCTION

The magnetoelectric (ME) effect, defined as an electric polarization response of a material to an applied magnetic field, is of both fundamental and technological importance.<sup>1</sup> This effect has been a hot research topic in recent years due to its potential applications in solid-state, self-powered ME devices. These include magnetic field sensors, current sensors, and speed sensors, to name a few.<sup>2</sup> To date, numerous single-phase and multiphase ME materials have been reported.<sup>3–9</sup> Among them, multiphase materials in forms of two-phase magnetostrictive-piezoelectric laminated composites or three-phase polymer-bonded magnetostrictive-piezoelectric laminated composites have attracted particular interest because of their naturally stronger ME effect characterized by larger ME voltage coefficient ( $\alpha_V$ ) and higher detection sensitivity. Typical examples comprise laminated composites of  $\text{Tb}_{1-x}\text{Dy}_x\text{Fe}_{2-y}$  (Terfenol-D) giant magnetostrictive alloy or its polymer-bonded composites and  $\text{Pb}(\text{Zr,Ti})\text{O}_3$  (PZT) piezoelectric ceramic or  $(1-x)\text{Pb}(\text{Mg}_{1/3}\text{Nb}_{2/3})\text{O}_{3-x}\text{PbTiO}_3$  (PMN-PT) piezoelectric single crystal or their polymer-bonded composites. The reported  $\alpha_V$  values are in the range of 20–110 mV/Oe and the detection sensitivities are typically down to  $10^{-5}$  Oe.<sup>4–9</sup> The high ME effect in these multiphase materials essentially

originates from the efficient stress-mediated ME coupling interaction between the magnetostrictive and piezoelectric material phases.

While the existing ME multiphase materials are effective and useful, the so-called high-performance piezoelectric phase (i.e., PZT or PMN-PT) contains a considerable amount of lead (Pb). In fact, Directive 2002/95/EC on the Restriction of the use of Certain Hazardous Substances in Electrical and Electronic Equipment (RoHS) and Directive 2002/96/EC on Waste Electrical and Electronic Equipment (WEEE) have expelled lead from many commercial applications and materials (e.g., from solder, glass, and pottery glaze) in Europe owing to concerns regarding the pollution on the environment and its toxicity to humans.<sup>10,11</sup> There is a global tendency to abandon the use of lead-based piezoelectric materials. Therefore, lead-free piezoelectric ceramics, which do not give rise to lead contamination and hazards, have undergone an intensive worldwide search in recent years in order to find good candidates to replace the commonly used lead-based piezoelectric materials.<sup>12–14</sup>

In response to the needs, we have prepared a perovskite-type lead-free piezoelectric ceramic  $(\text{Bi}_{1/2}\text{Na}_{1/2})\text{TiO}_3$ - $(\text{Bi}_{1/2}\text{K}_{1/2})\text{TiO}_3$ - $\text{BaTiO}_3$  (abbreviated as BNKT-BT) and measured attractive piezoelectric properties in comparison with the conventional PZT or PMN-PT lead-based piezoelectric materials (Table I).<sup>15</sup> As this ceramic can be treated as a prototype material in the lead-free piezoelectric ceramic community, it is expected that a reasonably high

<sup>a)</sup>Electronic mail: yanmin\_jia@yahoo.com.cn

TABLE I. Physical properties of BNKT–BT lead-free piezoelectric ceramic and Terfenol-D giant magnetostrictive alloy. The properties of some major lead-based piezoelectric materials, including PZT-5H soft ceramic, PZT-8 hard ceramic, and <001>-oriented PMN–PT single crystal, are also included for comparison with BNKT–BT.

	$d_{33}$ or $q_{33}$ (pm/V or nm/A)	$d_{31}$ or $q_{31}$ (pm/V or nm/A)	$g_{31}$ (mV m/N)	$s_{33}^E$ or $s_{33}^H$ (pm <sup>2</sup> /N)	$s_{11}^E$ or $s_{11}^H$ (pm <sup>2</sup> /N)	$s_{12}^E$ or $s_{12}^H$ (pm <sup>2</sup> /N)	$s_{13}^E$ or $s_{13}^H$ (pm <sup>2</sup> /N)
BNKT–BT	170	−40	−5.7	8.5	8.6	−2.0 <sup>c</sup>	4.3
PKI-552 <sup>a</sup>	550	−270	−9.0	20.2	15.9	−4.9	—
PKI-804 <sup>a</sup>	240	−100	−10.8	13.2	10.6	−2.7	—
PMN–PT <sup>b</sup>	2000	−1395	−23.8	57.7	57.3	−34.7	−23.6
Terfenol-D	11	−5.3	—	40	125	−37.5	−17

<sup>a</sup>Cited from Ref. 16.

<sup>b</sup>Cited from Ref. 17.

<sup>c</sup>Estimated value.

ME effect can be realized in BNKT–BT-based ME materials so as to enable green ME device technology. In this article, we describe the structure, fabrication, and working principle of a two-phase laminated composite with all phases environmentally friendly based on Terfenol-D giant magnetostrictive alloy and BNKT–BT lead-free piezoelectric ceramic (Fig. 1) as well as report experimentally and theoretically a high ME effect in such a composite with great values in green ME devices.

## II. STRUCTURE, FABRICATION, AND WORKING PRINCIPLE

Figure 1 illustrates the structure of the two-phase laminated composite of Terfenol-D and BNKT–BT. The composite consists of one layer of thickness-polarized BNKT–BT disk sandwiched between two identical layers of thickness-magnetized Terfenol-D disk along the thickness direction.

The BNKT–BT disk, 10 mm in diameter and 1 mm thick and with its polarization ( $P$ ) direction oriented in the thickness direction, was prepared in-house using the conventional mixed oxide technique.<sup>15</sup> Commercially available powders of Bi<sub>2</sub>O<sub>3</sub>, Na<sub>2</sub>CO<sub>3</sub>, K<sub>2</sub>CO<sub>3</sub>, BaCO<sub>3</sub>, and TiO<sub>2</sub> with purities higher than 99% were used as the starting materials. The powders were weighted according to the compositional formula of (Bi<sub>1/2</sub>Na<sub>1/2</sub>)TiO<sub>3</sub>–(Bi<sub>1/2</sub>K<sub>1/2</sub>)TiO<sub>3</sub>–BaTiO<sub>3</sub> and then mixed in alcohol using Y<sub>2</sub>O<sub>3</sub>-stabilized zirconia balls for 10 h. Calcination of the mixture was conducted at 800 °C for 1 h. The resulting mixture was ball-milled in alcohol for 10 h. After drying, the ball-milled powder was mixed thoroughly with a PVA binder solution for granulation. The granulated

powders were pressed uniaxially into a disk and sintered at 1170 °C for 2 h in an air atmosphere. The sintered disk was covered with silver electrodes on the two major surfaces, and polarization was imparted using these two electrodes in a silicone oil bath at 80 °C under 4.5 kV/mm for 5 min. The piezoelectric properties of the polarized BNKT–BT disk were measured according to the procedures stated in the IEEE Standard on Piezoelectricity.<sup>4</sup> Table I shows the measured properties of our BNKT–BT ceramic, together with those of some major lead-based piezoelectric materials, such as PZT-5H soft ceramic,<sup>16</sup> PZT-8 hard ceramic,<sup>16</sup> and <001>-oriented PMN–PT single crystal,<sup>17</sup> for comparison. It is clear that our BNKT–BT ceramic has properties comparable to the conventional lead-based materials.

The Terfenol-D disks, with the composition of Tb<sub>0.3</sub>Dy<sub>0.7</sub>Fe<sub>1.92</sub>, were commercially supplied with the dimensions the same as the BNKT–BT disk (Baotou Rare Earth Research Institute, China). They had the highly magnetostrictive [112] crystallographic axis along the thickness direction and thus magnetization ( $M$ ) was relatively easy in this direction. Their magnetostrictive properties are summarized in Table I.<sup>18</sup>

To construct the Terfenol-D/BNKT–BT/Terfenol-D laminated composite (Fig. 1), a BNKT–BT disk was bonded between two Terfenol-D disks along the thickness direction using a silver-loaded epoxy adhesive (Chemence Ionacure SL65) under a pressure of 10 MPa at 40 °C for 4 h to ensure good mechanical coupling between disks. The electrical wires were connected to the leads extended from the two electrodes of the BNKT–BT disk to form the output terminals.

The working principle of our laminated composite (Fig. 1) is essentially based on the product-property of the magnetostrictive effect in the Terfenol-D disks and the piezoelectric effect in the BNKT–BT disk, which are mediated by an effective mechanical coupling. In more detail, applying an ac magnetic field ( $H_3$ ) to the thickness direction of the composite produces planar magnetostrictive strains along the plane of the Terfenol-D disks, leading to planar stresses on the sandwiched BNKT–BT disk and causing it to produce thickness piezoelectric voltage ( $V_3$ ). For sensor applications, we analyze the composite by assuming that it is mechanically free in the 3-direction (i.e., stresses vanish in the 3-direction) and that it operates at frequencies well below its fundamental

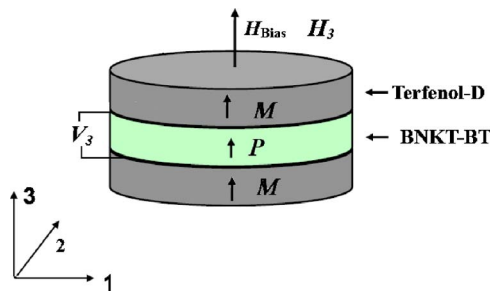


FIG. 1. Schematic diagram of our laminated composite. The arrow  $M$  and  $P$  represent the magnetization and polarization directions, respectively.

shape resonance. As the Terfenol-D disks are relatively thin and have the  $M$  direction oriented along their thickness in the 3-direction, deformations are essentially along the plane in the 1- and 2-directions.

An averaging method is used for deriving effective material parameters of this composite.<sup>21</sup> We can ignore any flexural deformations of the layers. The magnetostrictive phase is assumed to have a cubic symmetry and is described by the following equations:

$${}^mS_i = {}^ms_{ij}{}^mT_j + {}^mq_{ki}{}^mH_k, \quad (1a)$$

$${}^mB_k = {}^mq_{ki}{}^mT_i + {}^m\mu_{kn}{}^mH_n, \quad (1b)$$

where  ${}^mH_k$  and  ${}^mB_k$  are the vector components of magnetic field and magnetic induction;  ${}^mS_i$  and  ${}^mT_j$  are strain and stress tensor components of the magnetostrictive phase;  ${}^ms_{ij}$  and  ${}^mq_{ki}$  are compliance and piezomagnetic coefficients; and  ${}^m\mu_{kn}$  is the permeability matrix. This equation may be considered in particular as a linearized equation describing the effect of magnetostriction.

For the polarized piezoelectric phase with the symmetry  $\infty m$ , the piezoelectric constitutive equations can be written as following:

$${}^pS_i = {}^ps_{ij}{}^pT_j + {}^pd_{ki}{}^pE_k, \quad (2a)$$

$${}^pD_k = {}^pd_{ki}{}^pT_i + {}^p\epsilon_{kn}{}^pE_n, \quad (2b)$$

where  ${}^pE_k$  and  ${}^pD_k$  are the vector components of electric field and electric displacement;  ${}^pS_i$  and  ${}^pT_j$  are strain and stress tensor components of the piezoelectric phase;  ${}^ps_{ij}$  and  ${}^pd_{ki}$  are compliance and piezoelectric coefficients; and  ${}^p\epsilon_{kn}$  is the permittivity matrix.

Assuming in-plane mechanical connectivity between the two phases with appropriate boundary conditions, ME voltage coefficient can be obtained by solving Eqs. (1a), (1b), (2a), and (2b). Previous models assumed ideal coupling at the interface. Here we introduce an interface coupling parameter  $k = ({}^pS_i - {}^pS_{i0}) / ({}^mS_i - {}^mS_{i0})$  that describes the actual

boundary conditions,<sup>19</sup> where  ${}^pS_{i0}$  is the strain with no friction. The  $k$  value is 1 for ideal coupling and is 0 for the case with no friction. The tri-layer is considered as homogeneous and the behavior is described by the following equations containing effective parameters for the composites:<sup>19</sup>

$$S_i = s_{ij}T_j + d_{ki}E_k + q_{ki}H_k,$$

$$D_k = d_{ki}T_i + \epsilon_{kn}E_n + \alpha_{kn}H_n, \quad (3)$$

$$B_k = q_{ki}T_i + \alpha_{kn}E_n + \mu_{kn}H_n,$$

where  $E_k$ ,  $D_k$ ,  $H_k$ , and  $B_k$  are the vector components of electric field, electric displacement, magnetic field, and magnetic induction, respectively;  $S_i$  and  $T_j$  are strain and stress tensor components;  $s_{ij}$ ,  $d_{ki}$ , and  $q_{ki}$  are effective compliance, piezoelectric, and piezomagnetic coefficients, respectively; and  $\epsilon_{kn}$ ,  $\mu_{kn}$ , and  $\alpha_{kn}$  are effective permittivity, permeability, and ME coefficients, respectively. The effective parameters for the composite are obtained by solving Eqs. (1a), (1b), and (3). The mechanical strain and stress for tri-layer and homogeneous material are assumed to be the same, and the electric and magnetic vectors are determined using open and closed circuit conditions.

Magnetoelectric coupling is estimated from the induced field  $\delta E$  across the sample that is subject to an ac magnetic-field  $\delta H$  in the presence of a bias field  $H$ . The longitudinal ME voltage coefficient  $\alpha'_{E,33} = \delta E_3 / \delta H_3$  is given by:<sup>20</sup>

$$\alpha'_{E,33} = \frac{-\alpha_{33}(s_{33} + s_{c33}) - d_{33}q_{33}}{\epsilon_{33}(s_{33} + s_{c33}) - (d_{33})^2}. \quad (4)$$

The compliance of the clamp system is represented by  $s_{c33}$ , with zero compliance for rigidly clamped samples and infinite compliance for unclamped samples. In our experiment, the sample was unclamped, so it was under free boundary condition ( $T_1 = T_2 = T_3 = 0$ ).

Under free boundary condition,  $s_{33} \ll s_{c33} \rightarrow \infty$ , we can obtain<sup>19,20</sup>

$$\begin{aligned} \alpha'_{E,33} &= \frac{-\alpha_{33}}{\epsilon_{33}} = \frac{-2\mu_0kv(1-v){}^pd_{31}{}^mq_{31}}{2({}^pd_{31})^2(1-v)k + {}^p\epsilon_{33}[({}^ps_{11} + {}^ps_{12})(v-1) - kv({}^ms_{11} + {}^ms_{12})]} \\ &\times \frac{[({}^ps_{11} + {}^ps_{12})(v-1) - kv({}^ms_{11} + {}^ms_{12})]}{[\mu_0(v-1) - {}^m\mu_{33}v][kv({}^ms_{11} + {}^ms_{12}) - ({}^ps_{11} + {}^ps_{12})(v-1)] + 2({}^mq_{31})^2kv^2}, \end{aligned} \quad (5)$$

where  $v = v_p / (v_p + v_m)$  and  $v_p$  and  $v_m$  denote the volume of piezoelectric phase and magnetostrictive phase, respectively. If we assumed  $\mu_{33,m} / \mu_0 = 1$  and  $k = 1$ , the ME coefficient  $\alpha'_{E,33}$  is<sup>20</sup>

$$\alpha'_{E,33} = \frac{-2v(v-1){}^pd_{13}{}^mq_{31}}{({}^ms_{11} + {}^ms_{12}){}^p\epsilon_{33}v + ({}^ps_{11} + {}^ps_{12}){}^p\epsilon_{33}(1-v) - 2({}^pd_{13})^2(1-v)}. \quad (6)$$

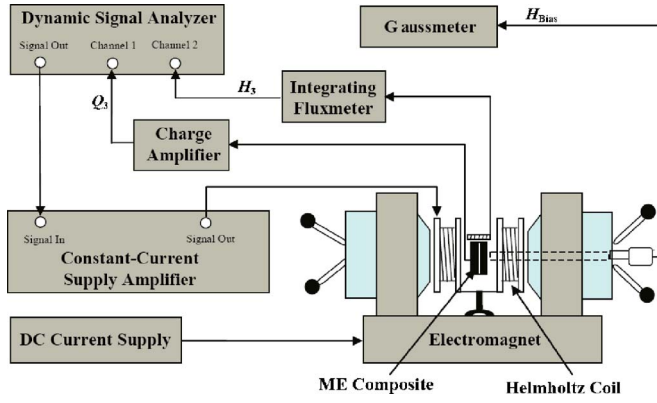


FIG. 2. Schematic diagram of the ME measurement setup.

This equation is the same form with the expression for longitudinal ME voltage coefficient by Harshe *et al.*<sup>21–23</sup> Substituting the corresponding material and geometric parameters of our samples into Eq. (6), the ME coefficient  $\alpha_V$  is  $\sim 32.1$  mV/Oe under free boundary condition.

### III. MEASUREMENTS

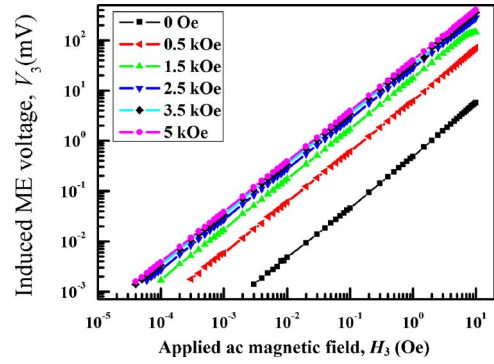
The ME effect of the fabricated composite was characterized at room temperature and with zero stress bias using an automated ME measurement setup shown in Fig. 2. The ME voltage ( $V_3$ ) induced in the composite was measured under different combinations of ac magnetic field strength ( $H_3$ ), dc magnetic bias level ( $H_{\text{Bias}}$ ), and ac magnetic field frequency ( $f$ ) in the ranges of  $3 \times 10^{-5}$ – $10$  Oe, 0–5.5 kOe, and 1–20 kHz, respectively.  $H_3$  was provided by a Helmholtz coil driven by a dynamic signal analyzer (Ono Sokki CF5220) via a constant-current supply amplifier (AE Techtron 7572).  $H_{\text{Bias}}$  was supplied by a U-shaped electromagnet (Mytem PEM-8005K) controlled by a dc current supply (Sorensen DHP200–15).  $H_3$  and  $H_{\text{Bias}}$  were monitored *in situ* by a pick-up coil connected to an integrating fluxmeter (Walker MF-10D) and a Gaussmeter (F. W. Bell 7030), respectively.  $V_3$  was determined from the measured charges ( $Q_3$ ) and capacitances ( $C$ ) of the BNKT–BT disk in the composite based on the relationship

$$V_3 = \frac{Q_3}{C}, \quad (7)$$

where  $Q_3$  and  $C$  were acquired by a charge amplifier (Kistler 5015A) and an impedance analyzer (Agilent 4294A), respectively. All quantities were sampled and recorded by the dynamic signal analyzer and stored in a computer. The dependence of the ME voltage coefficient ( $\alpha_V$ ) on both  $H_{\text{Bias}}$  and  $f$  was established from the slope of the corresponding  $V_3$ – $H_3$  plot.

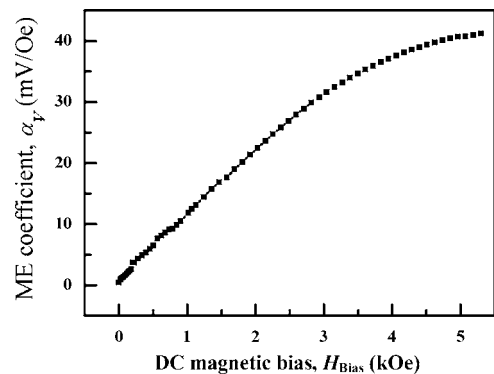
### IV. RESULTS AND DISCUSSION

Figure 3 shows the induced ME voltage ( $V_3$ ) as a function of applied ac magnetic field ( $H_3$ ) for various dc magnetic biases ( $H_{\text{Bias}}$ ) at the frequency of 1 kHz. It is seen that  $H_3$  has good linear responses to  $H_3$  in the entire  $H_3$  range of  $3 \times 10^{-5}$ – $10$  Oe for all  $H_{\text{Bias}}$ . The observation also indicates the high detection sensitivity nature of our composite al-

FIG. 3. Induced ME voltage ( $V_3$ ) as a function of applied ac magnetic field ( $H_3$ ) for various dc magnetic biases ( $H_{\text{Bias}}$ ) at the frequency of 1 kHz.

though it is subject to an  $H_3$  as small as  $3 \times 10^{-5}$  Oe. A further improved detection sensitivity of  $10^{-6}$ – $10^{-7}$  Oe is practically viable by shielding the magnetic noises and improving the composite quality. It is noted that the greatest  $V_3$ – $H_3$  response occurs at  $H_{\text{Bias}}$  of 5 kOe. From the slope of the  $V_3$ – $H_3$  plot at  $H_{\text{Bias}}$  = 5 kOe, the ME voltage coefficient ( $\alpha_V$ ) is determined to be 40.7 mV/Oe. Based our calculation,  $\alpha_V$  is 32.1 mV/Oe under free boundary condition. The experimental result is in good accordance with the prediction. The slight discrepancy may be due to in front of the roughness of each layer, the small difference of material constants of Terfenol-D between the cited value and the practical value,<sup>18</sup> the thickness and strength of the interface layer between the piezoelectric layer and magnetostrictive layer,<sup>24</sup> the pyroelectric effect of the ME composite,<sup>25,26</sup> etc. Nevertheless, we can approximately and simply estimate the magnitude of the ME coefficient for laminated composites through this model. Consequently, this  $\alpha_V$  and its associated detection sensitivity are comparable to those of most major two- or three-phase lead-based ME laminated composites, where  $\alpha_V$  of 20–110 mV/Oe and detection sensitivity of  $10^{-5}$  Oe are commonly achieved.<sup>4–9</sup>

Figure 4 shows the dependence of the ME voltage coefficient ( $\alpha_V$ ) on dc magnetic bias ( $H_{\text{Bias}}$ ) at the frequency of 1 kHz. The values of  $\alpha_V$  are obtained from the slopes of the  $V_3$ – $H_3$  plots in Fig. 3 at various  $H_{\text{Bias}}$ . It is interesting to note that  $\alpha_V$  increases linearly over a broad range of  $H_{\text{Bias}}$  from 0 to 3 kOe; it then tends to deviate from this linear relationship and reaches the technical maximum value of 40.7 mV/Oe at

FIG. 4. Dependence of ME voltage coefficient ( $\alpha_V$ ) on dc magnetic bias ( $H_{\text{Bias}}$ ) at the frequency of 1 kHz.



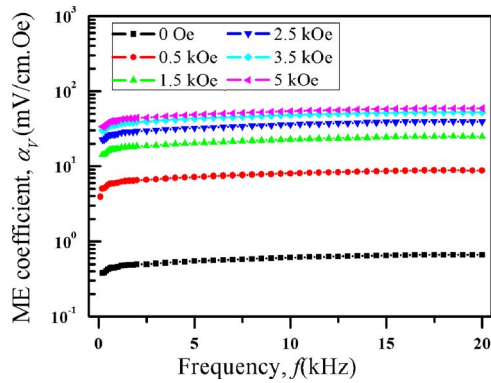


FIG. 5. Frequency ( $f$ ) dependence of the ME voltage coefficient ( $\alpha_V$ ) under different dc magnetic biases ( $H_{\text{Bias}}$ ).

5 kOe due to the saturation effect in the Terfenol-D disks.<sup>18</sup> This low-field linear range, to a certain extent, is broader than some major two- or three-phase lead-based ME laminated composites of less than 1 kOe.<sup>4-9</sup> The composite is a good candidate for use in dc ME sensors, besides the generally studied topic on the ac ME effect.<sup>27</sup>

Figure 5 shows the frequency ( $f$ ) dependence of the ME voltage coefficient ( $\alpha_V$ ) under different dc magnetic biases ( $H_{\text{Bias}}$ ). It is obvious that  $\alpha_V$  has flat responses in the measured frequency range of 0.1–20 kHz at all  $H_{\text{Bias}}$  with no remarkable dispersion of the ME effect. This suggests that our composite can be fabricated as a broadband, solid-state, lead-free ME device for  $f$  up to and, probably, beyond 20 kHz. For further improving the dynamic performance of the composite, preparation of a three-phase polymer-bonded version, instead of the current two-phase version, is strongly recommended.<sup>4-9</sup>

## V. CONCLUSION

In summary, a high ME effect has been found experimentally and theoretically in environmentally friendly laminated composites consisting of one BNKT–BT lead-free piezoelectric ceramic disk sandwiched between two Terfenol-D giant magnetostrictive alloy disks in the thickness direction. Besides its healthy nature, the results have demonstrated that this composite possesses a high  $\alpha_V$  of 40.7 mV/Oe at an optimal  $H_{\text{Bias}}$  of 5 kOe for a wide frequency range of 1–20 kHz, an excellent linear relationship between  $V_3$  and  $H_3$  for  $H_3$  varying dynamically from  $3 \times 10^{-5}$  to 10 Oe under different  $H_{\text{Bias}}$  of 0–5 Oe, and a good linearity between  $\alpha_V$  and  $H_{\text{Bias}}$  for  $H_{\text{Bias}}$  extending to 3 kOe. All these performances are comparable to most major two- or three-phase lead-based ME laminated composites, suggesting promising applications of the composite in green ME devices.

## ACKNOWLEDGMENTS

This work was supported by the 863 High Technology and Development Project of the People's Republic of China (Grant No. 2006AA03Z107), the Natural Science Foundation of China (Grant Nos. 50432030 and 50602047), Shanghai Municipal Government (Grant No. 05JC14079 and 06DZ05116), and the Research Grants Council of the HKSAR Government (Grant Nos. PolyU 5255/03E and PolyU 5122/05E).

- <sup>1</sup>L. D. Landau and E. Lifshitz, *Electrodynamics of Continuous Media* (Pergamon, Oxford, 1960).
- <sup>2</sup>*Magnetic Field Sensors Roadmap* (National Institute of Standards and Technology, Gaithersburg, MD, 2003).
- <sup>3</sup>V. J. Folen, G. T. Rado, and E. W. Stalder, *Phys. Rev. Lett.* **6**, 607 (1961).
- <sup>4</sup>S. Dong, J. F. Li, and D. Viehland, *IEEE Trans. Ultrason. Ferroelectr. Freq. Control* **50**, 1236 (2003).
- <sup>5</sup>S. Dong, J. F. Li, and D. Viehland, *Appl. Phys. Lett.* **83**, 2265 (2003).
- <sup>6</sup>N. Nersessian, S. W. Or, and G. P. Carman, *IEEE Trans. Magn.* **40**, 2646 (2004).
- <sup>7</sup>S. S. Guo, S. G. Lu, Z. Xu, X. Z. Zhao, and S. W. Or, *Appl. Phys. Lett.* **88**, 182906 (2006).
- <sup>8</sup>S. W. Or and N. Cai, *Solid State Phenom.* **111**, 147 (2006).
- <sup>9</sup>T. Li, S. W. Or, and H. L. W. Chan, *J. Magn. Magn. Mater.* **304**, e442 (2006).
- <sup>10</sup>*Directive 2002/95/EC of the European Parliament and of the Council of 27 January 2003 on the Restriction of the Use of Certain Hazardous Substances in Electrical and Electronic Equipment (RoHS)* (Official Journal of the European Union) (2003).
- <sup>11</sup>*Directive 2002/96/EC of the European Parliament and of the Council of 27 January 2003 on Waste Electrical and Electronic Equipment (WEEE)* (Official Journal of the European Union) (2003).
- <sup>12</sup>T. Takenaka and H. Nagata, *Key Eng. Mater.* **157**, 57 (1999).
- <sup>13</sup>Y. Saito, H. Takao, T. Tani, T. Nonoyama, K. Takatori, T. Homma, T. Nagaya, and M. Nakamura, *Nature (London)* **432**, 84 (2004).
- <sup>14</sup>X. X. Wang, S. W. Or, X. G. Tang, H. L. W. Chan, P. K. Choy, and P. C. K. Liu, *Solid State Commun.* **134**, 659 (2005).
- <sup>15</sup>X. X. Wang, X. G. Tang, and H. L. W. Chan, *Appl. Phys. Lett.* **85**, 91 (2004).
- <sup>16</sup>*PZT Materials Data Sheet* (Piezo Kinetics, Inc., Bellefonte, PA, 2006).
- <sup>17</sup>J. Peng, H. Luo, T. He, H. Xu, and D. Lin, *Mater. Lett.* **59**, 640 (2005).
- <sup>18</sup>G. Engdahl, *Handbook of Giant Magnetostrictive Materials* (Academic, New York, 2000).
- <sup>19</sup>M. I. Bichurin, V. M. Petrov, and G. Srinivasan, *J. Appl. Phys.* **92**, 7681 (2002).
- <sup>20</sup>M. I. Bichurin, V. M. Petrov, and G. Srinivasan, *Phys. Rev. B* **68**, 054402 (2003).
- <sup>21</sup>G. Harshe, J. O. Dougherty, and R. E. Newnham, *Int. J. Appl. Electromagn. Mater.* **4**, 145 (1993).
- <sup>22</sup>M. Avellaneda and G. Harshe, *J. Intell. Mater. Syst. Struct.* **5**, 501 (1994).
- <sup>23</sup>G. Harshe, Ph.D. thesis, The Pennsylvania State University (1991).
- <sup>24</sup>C. W. Nan, G. Liu, and Y. H. Lin, *Appl. Phys. Lett.* **83**, 4366 (2003).
- <sup>25</sup>Y. K. Fetisov, A. A. Bush, K. E. Kamantsev, and G. Srinivasan, *Solid State Commun.* **132**, 319 (2004).
- <sup>26</sup>Y. K. Fetisova, A. A. Bush, K. E. Kamantsev, and G. Srinivasan, <http://arxiv.org/ftp/cond-mat/papers/0401/0401481.pdf>
- <sup>27</sup>J. G. Wan, J.-M. Liu, G. H. Wang, and C. W. Nan, *Appl. Phys. Lett.* **88**, 182502 (2006).

Journal of Applied Physics is copyrighted by the American Institute of Physics (AIP).  
Redistribution of journal material is subject to the AIP online journal license and/or AIP  
copyright. For more information, see <http://ojps.aip.org/japo/japcr/jsp>